Novel PCU cage diol peptides as potential targets against wild-type CSA HIV-1 protease: Synthesis, biological screening and molecular modelling studies

6 AUTHORS, INCLUDING:

Yasien Sayed
University of the Witwatersrand
35 PUBLICATIONS   461 CITATIONS

SEE PROFILE

Gert Kruger
University of KwaZulu-Natal
302 PUBLICATIONS   1,604 CITATIONS

SEE PROFILE

Mahmoud Soliman
University of KwaZulu-Natal
56 PUBLICATIONS   323 CITATIONS

SEE PROFILE
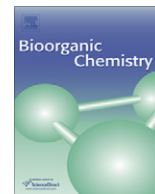
Glenn E M Maguire
University of KwaZulu-Natal
210 PUBLICATIONS   689 CITATIONS

SEE PROFILE

Pentacycloundecane derived hydroxy acid peptides: A new class of irreversible non-scissile ether bridged type isoster as potential HIV-1 wild type C-SA protease inhibitors

Rajshekhar Karpoormath [a], Yasien Sayed [c], Patrick Govender [b], Thavendran Govender [d], Hendrik G. Kruger [a], Mahmoud E.S. Soliman [e,*], Glenn E.M. Maguire [a,*]

[a] School of Chemistry, University of KwaZulu-Natal, Durban 4001, South Africa
[b] School of Biochemistry, University of KwaZulu-Natal, Durban 4001, South Africa
[c] Protein Structure-Function Research Unit, School of Molecular and Cell Biology, University of the Witwatersrand, Wits 2050, South Africa
[d] School of Pharmacy and Pharmacology, University of KwaZulu-Natal, Durban 4001, South Africa
[e] Department of Pharmaceutical Organic Chemistry, Faculty of Pharmacy, Zagazig University, Zagazig 44519, Egypt

ARTICLE INFO

ABSTRACT

Novel peptides incorporating the PCU derived hydroxy acid (5-hydroxy-4-oxahexacyclo[5.4.1.0^{2,6}.0^{3,10}.0^{5,9}.0^{8,11}]dodecane) were synthesized and their activity against the resistance-prone wild type C-South African (C-SA) HIV-protease is reported. The attachment of peptides and peptoids to the PCU derived hydroxy acid resulted in a series of structurally diverse promising HIV-1 protease inhibitors. Amongst the nine novel compounds, **16, 17, 20** and **23** gave IC$_{50}$ values ranging from 0.6 to 5.0 μM against the wild type C-SA HIV-1 protease enzyme. Docking studies and molecular dynamic (MD) simulations have been carried out in order to understand the binding mode of the PCU moiety at the active site of the HIV protease enzyme. A conserved hydrogen bonding pattern between the PCU derived hydroxy ether and the active site residues, ASP25/ASP25′, was observed in all active compounds.

© 2011 Elsevier Inc. All rights reserved.

1. Introduction

HIV is a global health problem and has become a major threat to the existence of the human race. It has already caused an estimated 25 million deaths worldwide and has generated profound demographic changes in the most heavily affected countries. In 2007 alone there were 2.7 million new HIV infections and 2 million HIV-related deaths worldwide [1]. The human immunodeficiency virus (HIV) encodes an aspartic protease (PR) that is essential for the formation of mature and infectious virions [2,3]. The HIV–PR is an established target in the chemotherapy of acquired immunodeficiency syndrome (AIDS) and intensive efforts have been directed to develop potent, orally available, peptidomimetic inhibitors for this enzyme [3–6]. At present, nine PR inhibitors have been approved by the FDA, and several others are now in clinical trials [6–8]. However, long-term anti-retroviral therapy for HIV infected patients promotes the emergence of resistance mutations of the HIV–PR, and consequently reduces

the clinical efficacy of these agents [9,10]. Thus, there is a continuing demand for newer mutant-resistant HIV–PR inhibitors. Fortunately, HIV–PR variants expressing resistance to inhibitors have also been derived in cell culture and therefore new classes of potential inhibitors can be evaluated against drug-resistant HIV strains [11].

Difficulties associated with drug-delivery have been observed mostly in peptide-based drugs due to their highly hydrophilic nature which results in poor membrane permeability [3,4,12]. A second limitation of peptide drugs is their susceptibility to in vivo degradation.

Over the past few years it was reported that the incorporation of polycyclic cage frameworks into biologically active molecules often improves the activity due to enhanced transport across cellular membranes [13–17]. The lipophilic nature of the cage skeleton also enables the molecules to cross the blood–brain barrier as well as the central nervous system (CNS) [14,18–20]. A second advantage of incorporating the cage skeleton into such compounds is an increased resistance to biodegradability [13]. The computational design [21–34], NMR elucidation [35–41] and biological studies [42–45] of several types of polycyclic cage molecules were previously reported in our group.

We have recently reported a family of PCU lactam peptides as potential HIV–PR inhibitors [33,34]. EASY–ROESY NMR experiments were used to determine crucial information about the 3D structure of these peptides in solution. The active inhibitors exhibited a turn of the peptide side chain that interacts with the cage protons. Docking of the cage peptides with the C-SA PR was also performed and a correlation of the binding energies with the IC_{50} inhibition results was evident. It was also demonstrated for the first time that the chirality of the PCU moiety was important for inhibition activity. Although the inhibitors approached activities in the nano molar range, it was clear that the need for better cage derived inhibitors should be explored. We decided to investigate a different PCU derivative as a potential transition state analog as well as to assess whether the introduction of peptoids may have a positive effect on the inhibition activity.

Considerable effort has been invested to improve the pharmacological properties of peptides, mainly by increasing their enzymatic stability while preserving the chemical moieties required for functional activity [46,47]. Peptoids represent a class of oligomeric compounds that closely mimic the natural structure of peptides and possess increased enzymatic stability as compared with homologous peptides. Peptoids are composed of N-substituted glycine (NSG) residues. The advances in the synthetic strategies used to prepare peptoid oligomers make them an attractive class of peptidomimetics [48–51].

Herein we report the synthesis and efficacy of peptide and peptoid based PCU hydroxy ether derived compounds as potential HIV-1 protease inhibitors. The strategy used for designing HIV protease inhibitors is to mimic the transition state analog of the Asp-induced enzyme cleavage thereby increasing the enzyme's affinity for the inhibitor over the peptide substrate.

Literature reports indicate that phenylalanine is the most common substituent at the S^1 subsite and it is found in 40% of Gag-Pol gene sequences of the virus [52]. According to literature, the $S^1/S^{1'}$ subsites accommodate hydrophobic substituents [53]. $S^2/S^{2'}$ and $S^3/S^{3'}$ subsites accommodate less hydrophobic substituents such as valine and alanine. It is postulated that inhibitors must have peptidic character with the scissile bond of the substrate being replaced by a non-cleavable bond [54,55]. The substrate specificity is determined by subsites located closely to the scissile bond. Primarily the $S^1/S^{1'}$ and $S^2/S^{2'}$ subsites being responsible for substrate recognition [56]. Based on this concept, we have designed and synthesized nine novel PCU derived hydroxy acid peptides and peptoid analogs. Variations of the amino acid sequence in the peptide chain were introduced. It was shown that the cage ether type bond of 2 is virtually non-hydrolysable under conditions that were harsher than physiological conditions [57].

Ghosh et al. developed nonpeptidyl ligands (Fig. 1) that displayed enhanced activity when cyclic ethers were incorporated into the structures [58–60]. The rationale behind using the cage ether is that when it is incorporated into a short peptide, this cyclic hydroxy ether moiety could perhaps serve as a cyclic ether transition state analog under protease conditions. The structural resemblance between the non-scissile cyclic ether and the cage ether is presented in Fig. 1, (structures 1 and 2). If this proposed interaction between the cage-peptide and the PR is possible, then it should result in effective inactivation of the PR [53].

This approach is a supplement to our recent report about the first family of PCU–lactam peptide HIV–PR inhibitors [33,34]. In that study, information about the 3D solution structure obtained from EASY–ROESY NMR techniques of the cage peptide could be correlated to the inhibitory activity of the peptide. A docking study followed by a QM/MM/MD study of the inhibitor/HIV–PR complex, suggested that the hydroxy lactam function of the PCU interacts with the Asp25/Asp25′ residues of the protease enzyme.
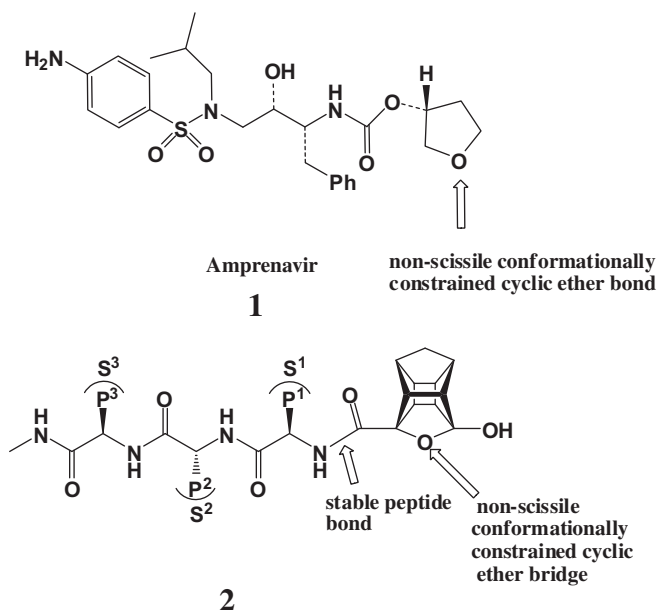

Fig. 1. Structure of the proposed 5-hydroxy-4-oxahexacyclo[5.4.1.0^{2,6}.0^{3,10}.0^{5,9}.0^{8,11}]dodecane peptide showing structural resemblance to the constrained cyclic ether bond of Amprenavir.

2. Material and methods

2.1. Experimental

Analytical analysis was performed on an Agilent 1100 HPLC (Waters Xbridge C18 150 mm × 4.6 mm × 5 μm) coupled to a UV detector (215 nm) and an Agilent VL ion trap mass spectrophotometer in the positive mode. Semi-preparative HPLC was carried out on a Shimadzu 8A instrument (Ace C18 150 mm × 21.2 mm × 5 μm) with a UV/VIS detector (215 nm) and automated fraction collector. A two-buffer system was employed, utilizing formic acid as the ion-pairing agent. Buffer A consisted of 0.1% formic acid/H_2O (v/v) and buffer B consisted of 0.1% formic acid/acetonitrile (v/v). High Resolution Electron Spray Ionization Mass Spectroscopic (HRESIMS) analysis was performed on a Bruker MicroTOF QII mass spectrometer in positive mode with an internal calibration. Microwave couplings were conducted on a Discovery CEM Liberty microwave peptide synthesizer. The coupling conditions of the peptide synthesizer were adapted from literature [33,34]. The ^{13}C NMR and ^{1}H NMR data were recorded on a Bruker AVANCE III 400 MHz spectrometer. Some samples were analyzed using a Bruker AVANCE III 600 MHz when higher sensitivity was required. Protease hydrolytic activity was measured by monitoring the relative decrease in absorbance at 300 nm using an Analytik Jena Specord 210 spectrophotometer. Optical rotations were measured at room temperature in dry methanol using a Perkin Elmer Polarimeter-Model 341. All IR spectra were recorded on a Perkin Elmer Spectrum 100 instrument with a universal ATR attachment. All the amino acids, resins and coupling reagents are commercially available and were purchased from GL Biochem (Shanghai) Ltd. Analytical grade solvents for synthesis were procured from Sigma–Aldrich (South Africa).

2.1.1. In vitro HIV-1 protease activity

The catalytic activity of the HIV-1 protease [34,61] was monitored following the hydrolysis of the chromogenic peptide substrate Lys-Ala-Arg-Val-Nle-p-nitro-Phe-Glu-Ala-Nle-NH$_2$. This substrate mimics the conserved KARVL/AEAM cleavage site

between the capsid protein and nucleocapsid (CA-p2) in the Gag polyprotein precursor .

For this study, the chromogenic substrate was synthesized using a Discovery CEM Liberty microwave peptide synthesizer on Rink amide resin. The substrate was cleaved from the resin and deprotected using 95:5 (v/v) TFA:TIS for 3 h. It was then precipitated using cold ether and purified *via* reverse phase semi-preparative HPLC on a Shimadzu instrument and characterized using the Bruker microTOF-Q II instrument (Table 1 in Supplementary information).

To determine the concentration of the compounds that resulted in 50% inhibition (IC_{50}) of HIV-1 protease enzyme activity, the protein (100 nM) and chromogenic substrate (50 µM) were added into a 120 µL microcuvette containing increasing concentrations of inhibitor in a pH 5.0 buffer (50 mM sodium acetate and 0.1 M NaCl). Protease hydrolytic activity was measured by monitoring the relative decrease in absorbance at 300 nm using an Analytik Jena Specord 210 spectrophotometer. Activity was standardized using commercially available drugs Atazanavir and Lopinavir. All cage peptides were soluble in the aqueous buffer solution. (pH = 5, 50 mM sodium acetate and 0.1 M NaCl).

2.1.2. General procedure for the synthesis of 5-hydroxy-4-oxahexacyclododecane-3-carboxylic acid, compound 15

Compound **15** was synthesized according to the previously reported method [57].

2.1.3. General procedure for manual SPPS loading of first amino acid to 2-chlorotrityl chloride resin [33,34]

Activated 2-chlorotrityl chloride resin (1 g, 1.33 mmol) was swelled in dry DCM (10 mL) for 10 min in a sintered glass reaction vessel. Fmoc-Amino acid-OH (3.99 mmol) in DCM (10 mL) and N,N-diisopropylethylamine (DIPEA) (6.65 mmol), was added to the resin and was mixed for 2 h with a stream of nitrogen bubbles. The solvent was removed by filtration and the resin was washed with DCM (3 × 10 mL). A few resin beads (∼5 mg) were removed from the reaction vessel and dried under vacuum for an hour. A solution of 20% piperidine in DMF was added to

the dried resin beads (1 mg) and left to stand for 20 min. General washing procedure for manual SPPS: After each step of SPPS the resin was washed with DCM (3 × 10 mL), DMF (3 × 10 mL) and DCM (3 × 10 mL).

2.1.4. General procedure for the synthesis of peptides using microwave power

Stock solutions of amino acids (0.2 mM), DIPEA (1 mM) and O-benzotriazole-N,N,N′,N′-tetramethyl-uronium-hexafluoro-phosphate (HBTU) (2 mM) were prepared and inserted to their appropriate reaction vessels on the peptide synthesizer. All peptides were synthesized on a 0.5 mmol scale using microwave power. The washing procedure was similar to the one used for manual SPPS. The standard coupling method for Arginine (Arg) was used for attachment of the second amino acid to the resin (1 g) preloaded with the first amino acid. The standard coupling method was used for subsequent reactions and for Fmoc deprotection [33,34,62]. The washing procedures were similar to those used for manual SPPS.

Final cleavage from the resin was performed manually. The resin bound peptide was washed with DCM (3 × 10 mL) in a reaction vessel while nitrogen was bubbled through the solution. A cleavage mixture of 0.5% (v/v) TFA and 95% (v/v) DCM was added to the dried resin while nitrogen was bubbled through the solution for 10 min. The resin was washed three times with the cleavage mixture and the cleaved peptide was removed by filtration and collected in a flask containing water (100 mL). The filtrate was extracted several times with DCM so as to remove the peptide from the water layer. DCM was removed under reduced pressure using a Teflon pump at 40 °C and affording the peptide as a white powder.

2.1.5. General procedure for the synthesis of peptoids [48–51]

Activated 2-chlorotrityl chloride resin (1.0 g, 1.33 mmol) was swelled in dry DCM (10 mL) for 10 min in a sintered glass reaction vessel. Bromoacetic acid (1.6 g, 11.51 mmol) and DIPEA (2 ml) were added to the resin and the mixture was bubbled for 2 h *via* a stream of nitrogen. The solvent was removed by

R^1 = Methyl
R^2 = Isopropyl
R^3 = Benzyl
R^4 = Pcu derived hydroxy acid
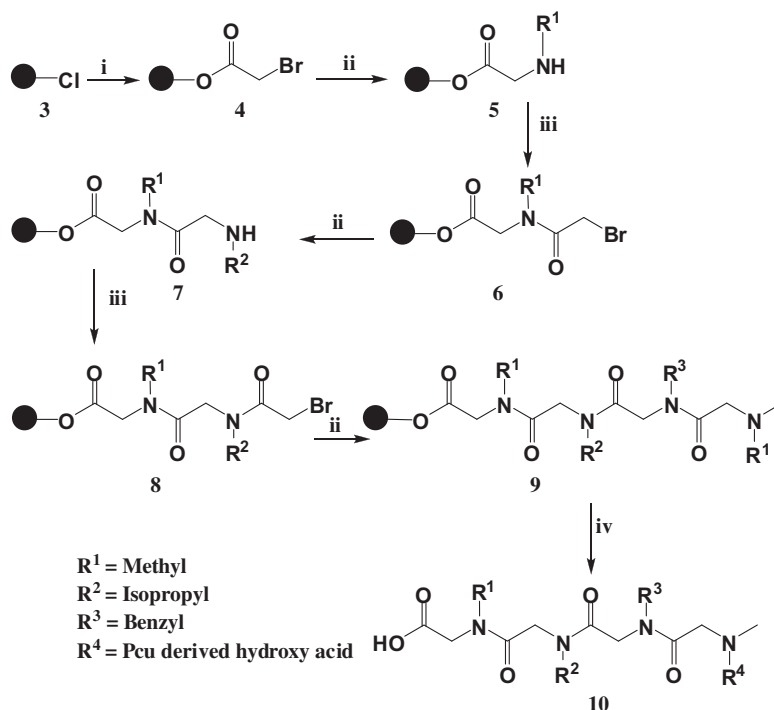
Scheme 1. General synthesis of peptoids: (i) = bromoacetic acid, DIPEA, dry DCM, (ii) = amine, DMF, (iii) = bromoacetic acid, DIC, DMF, and (iv) = 5% TFA, DCM.
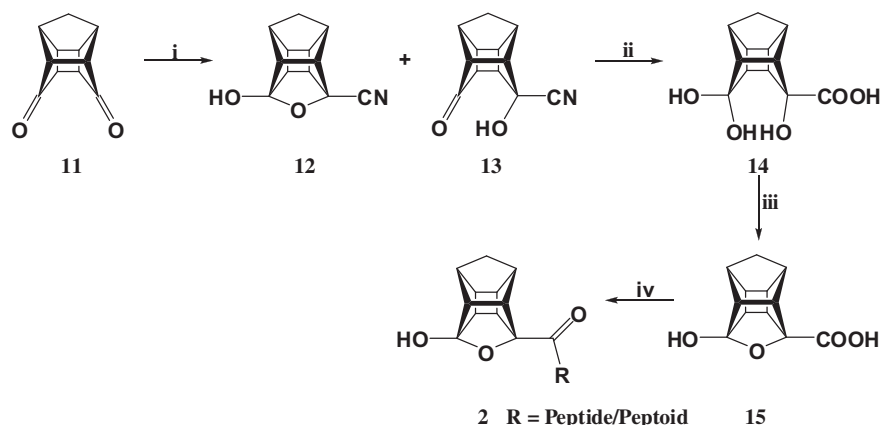
Scheme 2. Synthesis of 5-hydroxy-4-oxahexacyclo[5.4.1.0^{2,6}.0^{3,10}.0^{5,9}.0^{8,11}]dodecane peptide and peptoid analogs **2**: (i) = NaCN, CH$_3$COOH, H$_2$O, 0 °C, (ii) = conc. HCl, reflux, (iii) = 1,4-dioxane, reflux, and (iv) = HATU, DIPEA, DMF, RT.

filtration and the resin was washed with DCM (3 × 10 mL) and DMF (3 × 10 mL). A solution of the amine in DMF (1 M) was added to the reaction vessel and bubbled for 1 h with nitrogen. The solvent was removed by filtration and the resin was washed with DCM (3 × 10 mL) and DMF (3 × 10 mL). Bromoacetic acid (1.6 g, 11.51 mmol) and N,N′-diisopropylcarbodiimide (DIC) (2 ml) was then added and the mixture was added to the reaction vessel and bubbled for 2 h using nitrogen. The resin was washed as described previously followed by the addition of a solution of the amine (1 M), bromoacetic acid (1.6 g, 11.51 mmol) in DMF and DIC (2 ml). Final cleavage of the peptoid from the resin was carried out similarly as that of the peptides described previously.

2.1.6. General procedure for coupling of peptides and peptoids to 5-hydroxy-4-oxahexacyclododecane-3-carboxylic acid, compounds 16–24

The cleaved peptide (1.2 eq.) was dissolved in DCM (3 mL) followed by the addition of 5-hydroxy-4-oxahexacyclododecane-3-carboxylic acid[57] (1 equiv), HATU (2.5 equiv) in DMF (7 mL) and DIPEA (3 equiv) as a base. The mixture was left to stir at room temperature for 24 h. The product was evaporated to dryness under vacuum using a Teflon pump at 40 °C. A cleavage mixture (10 mL) of 95% (v/v) TFA and 5% (v/v) DCM was added to the coupled peptide and stirred for 24 h at room temperature to remove the N-Boc protecting group. The TFA was removed from the mixture by bubbling air through the peptide and the remaining DCM was removed under vacuum at 30 °C. The product was obtained as yellow oil which was purified by preparative HPLC.

2.1.6.1. Compound16. $[\alpha]_D^{20}$ = −23.81 (c 0.21 in MeOD); ^{1}H NMR (400 MHz, DMSO, 100 °C): δ 8.36 (q, J = 7.16, 5.40 Hz, 1H), 7.99 (dd, J = 9.12, 21.73 Hz, 1H), 7.44 (m, 1H), 7.23–7.09 (m, 5H), 4.59 (m, 1H), 4.24–4.15 (m, 2H), 3.05–2.89 (m, 2H), 2.73–2.56 (m, 3H), 2.45–2.43 (m, 6H) 1.97–1.92 (m, 1H), 1.79–1.76 (m, 1H),1.43 (d, J = 10.16 Hz, 1H), 1.27 (d, J = 7.32 Hz, 3H), 0.89–0.83 (m, 6H). ^{13}C NMR (100 MHz, DMSO, 100 °C): δ 170.8, 170.5, 170.4, 137.3, 129.3, 127.8, 126.2, 118.1, 89.5, 58.2, 57.9, 57.0, 56.1, 53.0, 48.4, 48.1, 47.4, 46.2, 46.0, 45.9, 42.7, 42.1, 40.9, 37.3, 31.1, 19.0, 18.1, 16.9, IR (neat): 3277.7, 2966.7, 1721.5, 1637.6, 1528.4, 1454.6, 1350.3, 1226.6, 1141.49, 911.2, 743.8, 698.9 cm^{-1}; HRESIMS (m/z): Calcd for C$_{29}$H$_{35}$N$_3$NaO$_7$ ([M+Na]$^{23+}$) 560.2367. Found 560.2351.

2.1.6.2. Compound 17. $[\alpha]_D^{20}$ = −27.27 (c 0.22 in MeOD); ^{1}H NMR (400 MHz, DMSO, 100 °C): δ 8.38 (m,1H), 8.04 (q, J = 9.06, 17.98 Hz, 1H), 7.41 (m, 1H), 7.25–7.10 (m, 5H), 4.62 (m, 1H), 4.24 (m, 1H), 3.84–3.71 (m, 2H), 3.36 (m, 1H), 3.06–2.92 (m, 2H),

2.73–2.57 (m, 3H), 2.45 (m, 5H), 1.97–1.95 (m, 1H), 1.80–1.77 (m, 1H),1.44 (d, J = 10.12 Hz, 1H), 0.89–0.84 (m, 6H). ^{13}C NMR (100 MHz, DMSO, 100 °C): δ 171.0, 170.5, 170.3, 137.3, 129.2, 127.9, 126.1, 118.1, 89.5, 79.1, 64.8, 58.2, 57.9, 57.2, 56.1, 53.0, 48.5, 48.1, 46.2, 46.0, 42.7, 42.1, 40.5, 37.3, 30.9, 19.0, 18.0, 15.1, IR (neat): 3288.5, 2965.7, 1728.2, 1638.4, 1524.0, 1327.6, 1206.3, 1138.62, 949.5, 905.3, 699.0 cm^{-1}; HRESIMS (m/z): Calcd for C$_{28}$H$_{33}$N$_3$NaO$_7$ ([M+Na]$^{23+}$) 546.2110. Found 546.2190.

2.1.6.3. Compound 19. $[\alpha]_D^{20}$ = −33.33 (c 0.21 in MeOD); ^{1}H NMR (400 MHz, DMSO, 100 °C): δ 8.54 (q, J = 6.46, 4.54 Hz, 1H), 8.02 (dd, J = 9.08, 20.28 Hz, 1H), 7.44 (m, 1H), 7.39–7.28 (m, 5H), 7.26–7.06 (m, 5H), 5.11 (s, 2H), 4.62 (m, 1H), 4.36 (m, 1H), 4.24 (m, 1H); 3.082–2.88 (m, 2H), 2.76–2.53 (m, 3H), 2.53–2.39 (m, 5H) 1.92 (m, 1H), 1.79 (d, J = 10.28 Hz, 1H),1.43 (d, J = 10.16 Hz, 1H), 1.32 (d, J = 7.32 Hz, 3H), 0.89–0.78 (m, 6H) ^{13}C NMR (100 MHz, DMSO, 100 °C): δ 172.2, 170.7, 170.6, 170.5, 170.3, 137.4, 135.9, 129.3, 128.4, 128.0, 127.9, 127.8, 126.2, 118.2, 89.6, 65.9, 58.3, 57.9, 57.0, 56.2, 53.1, 48.5, 48.2, 47.6, 46.3, 46.1, 45.9, 42.1, 41.0, 40.1, 37.4, 31.1, 19.0, 18.1, 16.7, IR (neat): 3287.8, 2964.4, 1714.9, 1640.5, 1524.1, 1327.2, 1205.2, 1138.4, 737.7, 697.0 cm^{-1}; HRESIMS (m/z): Calcd for C$_{36}$H$_{41}$N$_3$NaO$_7$ ([M+Na]$^{23+}$) 650.2837. Found 650.2828.

2.1.6.4. Compound 20. $[\alpha]_D^{20}$ = −20.00 (c 0.20 in MeOD); ^{1}H NMR (400 MHz, DMSO, 100 °C): δ 8.43 (m, 1H), 6.91 (q, J = 9.24, 1.68 Hz, 1H), 4.26–4.15 (m, 2H), 2.75–2.66 (m, 4H), 2.51 (m, 2H), 2.47 (m, 2H), 1.97–1.94 (m, 1H), 1.82 (q, J = 9.98, 3.14 Hz, 1H), 1.46 (d, J = 10.16 Hz, 1H), 1.27–1.24 (m, 3H), 0.87–0.77 (m, 6H). ^{13}C NMR (100 MHz, DMSO, 100 °C): δ 173.8, 170.4, 118.1, 89.6, 58.6, 57.9, 56.2, 55.9, 48.8, 48.1, 47.4, 46.3, 42.7, 42.1, 41.0, 40.0, 31.5, 19.0, 17.7, 16.9, 15.1, IR (neat): 3288.6, 2970.5, 1726.1, 1638.0, 1529.2, 1454.7, 1326.9, 1292.2, 1204.7, 1137.1, 992.5, 950.2, 906.4, 868.8, 641.7, 521.5 cm^{-1}; HRESIMS (m/z): Calcd for C$_{20}$H$_{26}$N$_2$NaO$_6$ ([M+Na]$^{23+}$) 413.1683. Found 413.1687.

2.1.6.5. Compound 22. $[\alpha]_D^{20}$ = −30.00 (c 0.21 in MeOD); ^{1}H NMR (400 MHz, DMSO, 100 °C): δ 8.14 (t, J = 7.98 Hz, 1H), 8.01 (d, J = 6.72 Hz, 1H), 7.84 (q, J = 8.90, 3.82 Hz, 1H), 7.36 (dd, J = 8.16, 2.32, 1H), 4.39–4.21 (m, 4H), 3.70 (m, 4H), 2.78–2.60 (m, 4H), 2.49–2.47 (m, 2H), 2.18 (q, J = 17.02, 8.25 Hz, 2H), 1.92–1.69 (m, 4H), 1.46 (d, J = 10.16 Hz, 1H), 1.43–1.48 (m, 1H), 1.19–1.16 (m, 3H), 1.10–1.02(m, 1H), 0.84–0.77 (m, 6H). ^{13}C NMR (100 MHz, DMSO, 100 °C): δ 173.9, 171.8, 170.9, 170.8, 170.4, 118.2, 89.6, 61.3, 58.4, 58.2, 56.6, 56.3, 54.6, 51.1, 48.6, 48.4, 48.0, 46.4, 46.1, 42.8, 42.2, 41.1, 37.0, 29.9, 27.7, 24.1, 18.1, 15.2, 11.1. IR (neat): 3281.1, 2967.6, 1717.7, 1633.9, 1525.4, 1452.1, 1330.4, 1205.7, 1138.8, 1056.7, 993.7, 950.4, 904.2, 868.6, 789.4, 640.8, 616.9 cm^{-1}. HRE-

SIMS (m/z): Calcd for $C_{29}H_{40}N_4NaO_{11}$ ([M+Na]$^{23+}$) 643.2586. Found 643.2579.

2.1.6.6. Compound 23.
^{1}H NMR (400 MHz, DMSO, 100 °C): δ 4.75–4.69 (m, 1H), 4.45–4.35 (m, 1H), 4.15 (s, 1H), 3.97–3.95 (m, 2H), 3.84 (d, J = 4.32 Hz, 1H), 3.01 (d, J = 16.76 Hz, 2H), 2.96–2.89 (m, 2H), 2.79 (d, J = 9.56 Hz, 1H), 2.68–2.56 (m, 2H), 2.47–2.34 (m, 4H), 1.83 (d, J = 10.08 Hz, 1H), 1.45 (d, J = 10.52 Hz 1H), 1.05–0.99 (m, 6H). ^{13}C NMR (100 MHz, DMSO, 100 °C): δ 170.7, 168.2, 118.6, 90.5, 58.3, 55.2, 49.1, 48.3, 46.7, 45.6, 42.9, 41.0, 41.6, 41.0, 40.8, 37.8, 35.2, 34.5, 20.7, 19.3, 18.7. IR (neat): 3358.2, 2968.3, 2866.4, 1728.1, 1603.1, 1460.6, 1405.6, 1335.5, 1290.9, 1195.7, 1134.4, 1068.2, 1002.7, 904.5, 868.5, 827.9, 741.8, 645.7, 538.9 cm^{-1}; HRESIMS (m/z): Calcd for $C_{20}H_{26}N_2NaO_6$ ([M+Na]$^{23+}$) 413.1683. Found 413.1682.

2.1.6.7. Compound 24.
^{1}H NMR (400 MHz, DMSO, 100 °C): δ 7.35–7.14 (m, 5H), 4.69–4.35 (m, 3H), 4.18–4.05 (m, 3H), 3.99–3.89 (m, 4H), 3.05–2.97 (m, 5H), 2.81–2.72 (m, 1H), 2.66–2.65 (m, 2H), 2.47 (s, 2H), 1.87–1.82 (m, 1H), 1.49–1.45 (m, 1H), 1.05–0.91 (m, 6H). ^{13}C NMR (100 MHz, DMSO, 100 °C): δ 170.6, 170.2, 169.0, 137.3, 128.4, 127.4, 118.7, 90.5, 58.7, 55.3, 48.6, 47.9, 45.6, 44.5, 42.9, 42.6, 41.8, 40.9, 35.2, 35.1, 20.33, 19.4, 19.2. IR (neat): 3332.8, 2971.8, 1731.5, 1629.7, 1453.7, 1405.5, 1343.5, 1291.8, 1197.6, 1135.9, 1075.7, 1007.0, 904.9, 868.7, 741.1, 630.7 cm^{-1}; HRESIMS (m/z): Calcd for $C_{29}H_{35}N_3NaO_7$ ([M+Na]$^{23+}$) 560.2367. Found 560.2358.

2.1.7. General procedure [63] for the synthesis of benzyl protected 5-hydroxy-4-oxahexacyclododecane peptides, 18 and 21
5-Hydroxy-4-oxahexacyclododecane peptide (1 eq) and benzybromide (2.5 eq) were dissolved in DMF (8 mL). Cesium carbonate (2 eq) was added to the solution at ambient temperature. After stirring for 2 h, saturated aqueous sodium bicarbonate (100 mL) was added to the solution and extracted with ethyl acetate (3 × 100 mL). The combined organic phases were washed with 5% aqueous citrate and saturated aqueous sodium chloride (100 mL) and dried over sodium sulfate. The solvent was evaporated, and the crude peptide was precipitated in cold ether and dried under reduced pressure. This crude product was further purified by preparative HPLC.

2.1.7.1. Compound 18.
$[\alpha]_D^{20}$ = −19.05 (c 0.21 in MeOD); ^{1}H NMR (400 MHz, DMSO, 100 °C): δ 8.32 (d, J = 7.36 Hz, 1H), 7.95 (q, J = 9.06, 17.34 Hz, 1H), 7.39 (m, 1H), 7.27–7.09 (m, 10H), 4.63 (m, 1H), 4.58 (m, 1H), 4.48–4.43 (m, 1H), 4.28–4.23 (m, 1H), 3.55 (s, 1H), 3.36 (m, 1H), 3.09–2.89 (m, 4H), 2.71–2.55 (m, 3H), 2.45 (m, 4H), 1.97–1.93 (m, 1H), 1.78 (d, J = 10.32 Hz, 1H), 1.43 (d, J = 10.12 Hz, 1H), 0.85–0.80 (m, 6H). ^{13}C NMR (100 MHz, DMSO, 100 °C): δ 172.7, 170.7, 170.4, 170.2, 137.4, 137.3, 129.2, 128.9, 128.1, 127.8, 126.3, 118.1, 89.5, 64.8, 58.2, 57.9, 56.9, 56.1, 53.3, 52.9, 48.5, 48.1, 46.2, 45.9, 42.7, 42.1, 40.9, 37.4, 37.3, 36.5, 31.1, 19.0, 17.8, 15.1, IR (neat): 3289.0, 2965.3, 1720.5, 1641.6, 1523.6, 1326.3, 1206.3, 1138.5, 906.4, 698.1 cm^{-1}; HRESIMS (m/z): Calcd for $C_{35}H_{39}N_3NaO_7$ ([M+Na]$^{23+}$) 636.2719. Found 636.2680.

2.1.7.2. Compound 21.
$[\alpha]_D^{20}$ = −33.33 (c 0.21 in MeOD); ^{1}H NMR (400 MHz, DMSO, 100 °C): δ 8.59 (t, J = 6.82 Hz, 1H), 7.38–7.30 (m, 5H), 7.13 (d, J = 1.40 Hz, 1H), 6.88 (q, J = 9.26, 3.78 Hz, 1H), 5.10 (s, 1H), 4.36–4.31 (m, 1H), 4.27–4.22 (m, 1H), 2.77–2.63 (m, 4H), 2.56–2.51 (m, 2H), 2.47 (m, 1H), 1.96–1.90 (m, 1H), 1.82 (q, J = 10.20, 5.60 Hz, 1H), 1.47 (d, J = 9.96 Hz, 1H), 1.31–1.29 (m, 3H), 0.85–0.81 (m, 3H), 0.77–0.73 (m, 3H). ^{13}C NMR (100 MHz, DMSO, 100 °C): δ 172.1, 170.4, 170.3, 135.8, 128.3, 128.0, 127.7, 118.1, 89.6, 65.9, 58.6, 57.9, 56.2, 55.9, 55.8, 48.8, 48.1, 47.5, 46.3, 46.0, 42.7, 42.1, 31.5, 19.0, 17.6, 16.7. IR (neat): 3286.7, 2966.8,

1742.8, 1643.5, 1524.4, 1455.5, 1347.2, 1203.2, 1160.4, 1138.8, 1052.4, 991.3, 949.3, 904.7, 738.0, 697.3, 640.9 cm^{-1}; HRESIMS (m/z): Calcd for $C_{27}H_{32}N_2NaO_6$ ([M+Na]$^{23+}$) 503.2153. Found 503.2150.

2.2. Computational simulations

2.2.1. Preparation of PCU derived peptide inhibitors
The structures of the cage-peptides/peptoids, **16–24**, were constructed and the geometry was optimized using the MMFF94 force field implemented in the Avogadro software [64]. Both diastereomers of the cage peptides were investigated. The minimized structures were then subjected to docking studies.

2.2.2. C-SA PR enzyme model system
Since the X-ray structure of the South African HIV-1 protease subtype C (C-SA) has not yet been reported, the initial 3D structure of the enzyme was taken from the reported X-ray data of subtype B HIV–PR (PDB accession code 1HXW) [10]. C-SA HIV–PR differs from subtype B at eight positions; T12S, I15V, L19I, M36I, R41K, H69K, L89M and I93L [61]. The X-ray crystallographic coordinates of 1HXW were modified as follows:

The original substrate included in the crystal structure, Ritonavir, and the crystallographic water molecules were removed and hydrogens were added to the system. Ionization states for ionizable amino acid residues were determined according to their standard pKa values. Mutations at eight positions, T12S, I15V, L19I, M36I, R41K, H69K, L89M and I93L were manually induced. Throughout this work, the modeled C-SA HIV–PR was used for docking and MD simulations. This constructed enzyme was successfully used in our previous study on cage lactam peptides [33,34].

2.2.3. Docking of the inhibitors into the C-SA PR model
The energy minimized inhibitors, **16–24** were used in docking simulations. The effect of ionization states of docked compounds to the binding scores has been discussed in the literature [65–67]. The ionization states of the cage-peptide inhibitors have not yet been determined experimentally. During docking, the neutral and ionized states (aliphatic amine and carboxylic acid groups of compounds to be docked were protonated and deprotonated, respectively) were considered and compared, separately. The simulations were performed under physiological pH conditions, which require the correct protonation state of ionizable groups. In particular, one of the aspartates (Asp25) of the catalytic site exhibits an increased pKa value of 5.2 in the inhibitor-bound protease [53] while no increased pKa was reported for the free form of the protease (pKa = 4.5) [68]. Therefore, a monoprotonated active site should be prevalent at physiological pH, and thus this protonation state was used throughout these docking studies. However, to ensure that the results of the simulations do not critically depend on the protonation state, a control simulation of a cage-bound CSA-HIV-1 protease with a deprotonated carboxylate oxygen of the Asp25/Asp25′ residues was also performed. We have previously reported that no significant difference was observed for docking of the cage lactam peptides with the different protonation states of the enzyme [33,34].

Docking studies were performed using the Autodock software [69]. Geisteger charges were computed and the Autodock atom types were defined using the Autodock Tools graphical user interface supplied by MGL Tools [70]. The Lamarckian Genetic Algorithm (LGA), which is considered one of the best docking methods available in Autodock [69,71] was employed. This algorithm yields superior docking performance compared to simulated annealing or the simple genetic algorithm and the other search algorithms available in Autodock. The docked conformations of
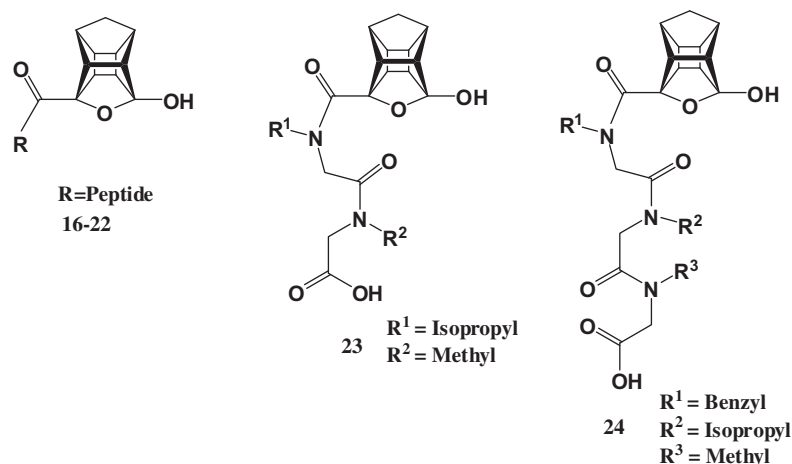
R¹ = Isopropyl
R² = Methyl
23

R=Peptide
16-22

R¹ = Benzyl
R² = Isopropyl
R³ = Methyl
24

Fig. 2. PCU–peptide and PCU–peptoid based inhibitors reported in this work.

R = Peptide / Peptoid
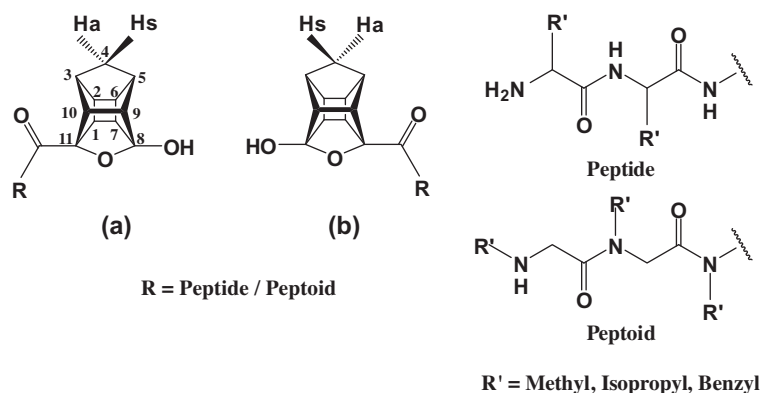
Peptide

Peptoid

R' = Methyl, Isopropyl, Benzyl

Fig. 3. Stereochemistry of the generic cage diastereomers (a) and (b).

each of the diastereomeric ligands were ranked into clusters based on the binding energy. The top ranked conformations were visually analyzed. The suitability of the constructed C-SA PR for docking experiments was tested with a control experiment in which Ritonavir, was docked into the active site of the modeled enzyme and compared to the X-ray crystal structure [54] of the Ritonavir-protease complex.

2.2.4. MD simulations of the inhibitor–enzyme complex

MD simulations were performed for the inhibitor–enzyme complex of the most active compound **20**. The diastereomer with

the best docked binding energy was used. Partial charges and the force field parameters for the inhibitor were generated using the Antechamber program [72] in the Amber10 package [73]. These were described by the general Amber force field (GAFF) [74]. All hydrogen atoms of the proteins were added using the Leap module in Amber10. The standard AMBER force field for bioorganic systems (ff03) [75] was used to describe the HIV PR enzyme parameters. Counter ions were added to neutralize the complex. Then, the system was solvated using atomistic TIP3P water [76] in a cubic box with 8.0 Å distance around the complex.

Table 1
Inhibition of wild type C-SA HIV-1 protease by PCU derived peptides (**16–22**) and peptoids (**23–24**).

Entry	Sr. no.	Compound (R)			MF	% Yield	C Log P	Binding energy[a]	IC$_{50}$ (μm)[b]
1	**16**	HO-Ala-Val-Phe-			$C_{29}H_{35}N_3O_7$	42	0.792	−7.01	2
2	**17**	HO-Gly-Val-Phe-			$C_{28}H_{33}N_3O_7$	54	0.483	−7.74	1
3	**18**	Bn-O-Ala-Val-Phe-			$C_{36}H_{41}N_3O_7$	46	2.623	−5.53	>60
4	**19**	HO-Phe-Val-Phe-			$C_{35}H_{39}N_3O_7$	38	2.210	−5.02	>60
5	**20**	HO-Ala-Val-			$C_{20}H_{26}N_2O_6$	68	−0.367	−8.98	0.6
6	**21**	Bn-O-Ala-Val-			$C_{27}H_{32}N_2O_6$	51	1.462	−6.54	60
7	**22**	HO-Ser-Ilu-Ala-Glu-			$C_{29}H_{40}N_4O_{11}$	62	−2.310	−4.62	>60
8	**23 (Peptoid)**	R¹ = isopropyl	R² = methyl		$C_{20}H_{26}N_2O_6$	57	0.138	−7.21	5
9	**24 (Peptoid)**	R¹ = benzyl	R² = isopropyl	R³ = methyl	$C_{29}H_{35}N_3O_7$	43	1.795	−6.75	>60
10		**Lopinavir**							0.025
11		**Atazanavir**							0.004

[a] Calculated with Autodock. The diastereomer with the lowest binding energy is reported here. The 3D structures of these docked complexes are available as Supplementary material.
[b] IC$_{50}$ = 50% inhibition constant. Standard deviations (SD) for all the compounds were ⩽2% of the reported IC$_{50}$ values.

The molecular dynamics package Amber10 [73] was used for the minimization and equilibration protocols. Cubic periodic boundary conditions were imposed and the long-range electrostatic interactions were treated with the particle-mesh Ewald method [77] implemented in Amber10 with a non-bonding cutoff distance of 10.0 Å. The energy minimization was first conducted using the steepest descent method in Amber10 for 1000 iterations switched to conjugate gradient for 2000 steps with a restraint potential of 2 kcal/mol Å^2 applied to the solute. Then the total system was freely minimized for 1000 iterations. For the equilibration and subsequent production run, the SHAKE algorithm [78] was employed on all atoms covalently bonded to a hydrogen atom, allowing for an integration time step of 2 fs. Harmonic restraints with force constants 2.0 kcal/mol Å^2 were applied to all solute atoms. A canonical ensemble (NVT) MD was carried out for 70 ps, during which the system was gradually annealed from 0 to 300 K using a Langevin thermostat with a coupling coefficient of 1.0/ps. Subsequently, the system was equilibrated at constant volume and temperature (300 K) with a 2 fs time step for 100 ps while maintaining the force constants on the restrained solute. With no restraints imposed, a production run was performed for 2 ns in isothermal isobaric (NPT) ensemble using a Berendsen barostat [79] with a target pressure of 1 bar and a pressure coupling constant of 2 ps. The coordinate file was saved every 1 ps and the trajectory was analyzed at every 1 ps using the Ptraj module implemented in Amber10.

3. Results and discussion

3.1. Synthesis, spectral characterization and biological activity

The cage peptides and peptoids were synthesized as described in the experimental section. In most cases, the peptides/peptoids were of sufficient purity to be coupled to the PCU derived hydroxy acid after lyophilization. The peptoid oligomers were synthesized *via* solid phase synthesis on activated 2-chlorotrityl chloride resin **3** by attaching bromoacetic acid in the presence of DIPEA in dry dichloromethane (DCM) affording compound **4**. Upon filtration, the amine solution in DMF was added and mixed under a stream of nitrogen bubbles to give compound **5**. The chain was elongated by coupling bromoacetic acid in the presence of *N,N′*-diisopropyl-carbodiimide (DIC). Similarly the corresponding amines were coupled to the extended chain followed by bromoacetic acid to give compounds **6–10**. The completed peptoids were cleaved from the resin using 5% trifluoroacetic acid (TFA) in DCM as illustrated in Scheme 1.

The cage hydroxy acid **15** [57] was synthesized from pentacycloundecane-8,11-dione **11** [80–82] which can be easily obtained from the photocyclization of the Diels–Alder adduct of cyclopentadiene and *p*-benzoquinone. A solution of the dione **11** in a mixture of water and acetic acid stirred in an ice bath is treated with an aqueous solution of sodium cyanide to form a mixture of the cyanohydrin (**12** and **13**) [57]. This cyanohydrin mixture when treated with concentrated hydrochloric acid gives the tri-hydroxy carboxylic acid **14** [57]. It should be noted that this cage acid is synthesised as a racemate. The resulting cage peptides are therefore a mixture of two diastereomers, Fig. 3a and b.

Tri-hydroxy carboxylic acid **14** was refluxed in 1,4-dioxane to give the desired hydroxy acid **15**. The peptides and peptoids obtained were coupled to **15** with HATU, DIPEA in DMF at ambient temperature as shown in Scheme 2.

The products **16–24** (Fig. 2) were isolated and purified as described in the experimental section. It was not possible to separate the diastereomeric mixtures by preparative HPLC. The correctness of the cage peptides and peptoids were confirmed with standard NMR and MS techniques. The purity of the peptides were determined with HPLC and were >98%.

The catalytic activity of the HIV-1 protease was monitored by following the hydrolysis of the chromogenic peptide substrate His-Lys-Ala-Arg-Val-Leu-Phe(p-NO$_2$)-Glu-Ala-Nle-Ser as described before [61]. The use of chromogenic substrates has been established for the determination of the HIV-1 protease inhibitors efficacy. The method is used to measure the protease activity by recording an decrease in absorbance as a result of the hydrolysis of a chromogenic substrate by the protease [83]. The inhibitory activities of the synthesized compounds were tested using an UV spectrophotometric assay in order to determine the IC$_{50}$ values for each compound. Biological results of the synthesized substrates are presented in Table 1.

As we have previously reported [34], it appears in general that the cage peptides exhibit very little cytotoxicity towards human cells.

According to previous literature reports, phenylalanine is the preferred substituent (P^1) at the S^1 subsite and it is found in 40% of *Gag-Pol* gene sequences of the virus [52]. Thus, we decided to synthesize sequences, with phenylalanine as the first amino acid (P^1 substituent), attached to the PCU cage. Even though the S^2/S$^{2′}$ and S^3/S$^{3′}$ pockets are also of a hydrophobic nature, both hydrophilic and hydrophobic side chains from the *Gag* and *Gag-Pol* polyproteins can occupy these sites. Based on literature and the HIV substrate sequence, we envisaged that either valine or alanine would be the best starting point in the peptide chain for binding at the S^2/S$^{2′}$ and S^3/S$^{3′}$ subsites [33,34].

It was observed that compound **16** (entry 1) showed a moderate inhibition of 2 μM (IC$_{50}$). For compound **17** (entry 2), the activity increased by onefold, where alanine was replaced by glycine at the proposed P^3/P$^{3′}$ position. When more hydrophobic bulky groups were incorporated as the P^3/P$^{3′}$ substituent, little or no inhibition activity was observed (compound **18**, entry 3 and **19**, entry 4). The reduced potency of these compounds could be as a result of the bulky hydrophobic residues occupying the S^3/S$^{3′}$ subsite. Since the S^1/S$^{1′}$ and S^3/S$^{3′}$ positions are located adjacent to one another in the *cis* configuration, incorporation of bulky substituents in both the subsites could alter the conformational arrangements which consequently reduces their binding affinity [6,53,56]. This possibility will be discussed with the presentation of the docking results.

To investigate if the PCU-cage is competing with phenylalanine for the S^1 subsite, phenylalanine was removed from peptide **16** (entry 1), to give compound **20** (entry 5). This resulted in a higher binding affinity and preference for the active site with an inhibitory activity of 0.6 μM (IC$_{50}$). This is a 2–4-fold greater activity than compounds **16** (entry 1) and **17** (entry 2), which suggests that PCU cage is indeed occupying the S^1 subsite. To examine the role of a hydrophobic group at S^3 subsite we synthesized compound **21** (entry 6) containing a benzyl protecting group on the C terminal of the peptide sequence. This reduced binding affinity to the active site and had no inhibitory affect. This result is similar to that of compound **18** (entry 3).

Compounds **22** (entry 7) containing PCU cage with the natural HIV protease substrate (PCU-EAIS) showed inhibition activity greater than 60 μM (IC$_{50}$). Oligomers of *N*-substituted glycines are known to be resistant to proteolysis [48–51]. Keeping this in mind compounds **23** (entry 8) and **24** (entry 9) were synthesized to mimic the peptide sequence of compound **20** (entry 5) and **16** (entry 1) respectively. Compound **23** (entry 8) showed inhibition activity of 5 μM (IC$_{50}$), which is approximately 10-fold less active, when compared to **20** (IC$_{50}$, 0.6 μM). No inhibition activity was observed for compound **24** (entry 9) as compared to compound **16** (entry 1).

From the compounds in Table 1 the best inhibition activity was obtained for compound **20** (entry 5). The activity is promising
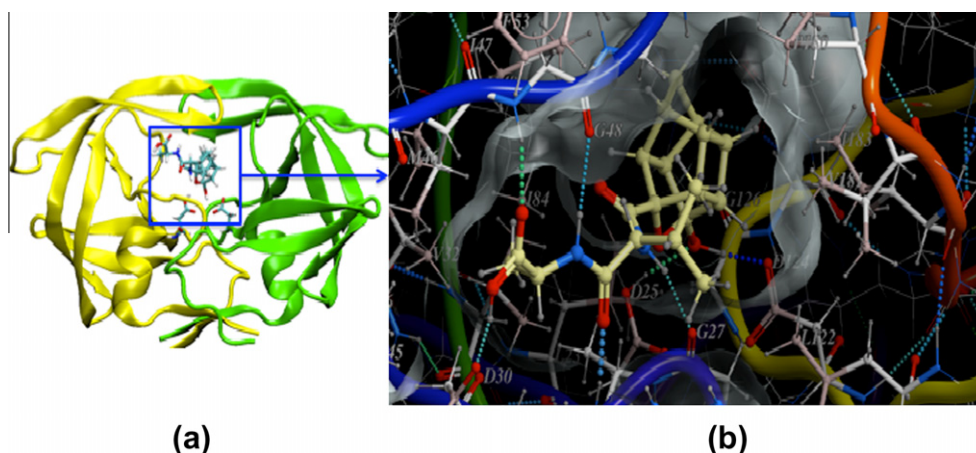
Fig. 4. (a) Lowest energy docked structure for compound **20** with C-SA HIV–PR. (b) A closer view showing the binding mode of compound **20** inside the C-SA HIV–PR active site. Some atoms are deleted for clarity. The two PR monomers are colored as the yellow and green ribbon. The inhibitor and the two Asp25 residues presented as colored sticks. The 3D presentations for computational results are available as PDB files with the Supporting information.

when compared with Lopinavir (entry 10) but almost two orders of magnitude less active than Atazanavir (entry 11). To further validate these experimental results, docking studies and MD simulations were performed on the most active compound.

3.2. Computational simulations

3.2.1. Docking and MD simulations

To obtain a better understanding of the molecular and biological behavior of the synthesized PCU–peptide inhibitors, we embarked on a computational investigation involving docking and MD simulations. First, the PCU–peptides were subjected to docking studies to explore their binding pattern; second MD simulations of the docked inhibitor enzyme complex were performed to provide a molecular view of the dynamic behavior of such inhibitors inside the enzyme active site over a suitable time

scale. Docking studies are used at different stages in drug discovery such as in the prediction of ligand–receptor complex structures and also to rank the ligand molecules based upon the binding energies of the corresponding ligand–enzyme complexes. Docking protocols aid in elucidation of the most energetically favorable binding mode of the ligand to the receptor. The objective of our docking study was to elucidate the potential interaction mode of the PCU–peptide derivatives with C-SA HIV PR and to see if a correlation between the binding energies and the observed IC_{50} results exists.

Docking of Ritonavir (co-crystallized inhibitor) with subtype B HIV–PR (PDB accession code 1HXW) [10] was previously performed [33,34] to evaluate the efficacy of Autodock for its use in docking experiments with this subtype as a target. Acceptable results were obtained. The interacting amino acids in the C-SA starting structure were conserved in the conformation of the enzyme
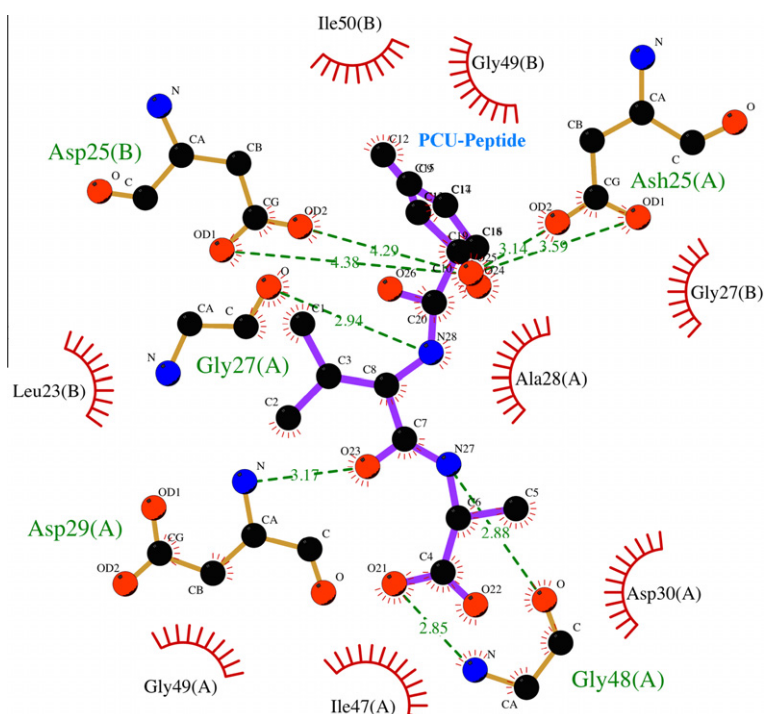

Fig. 5. Electrostatic and hydrogen bonding interaction between **20** and the nearby residues of C-SA HIV–PR active site. This plot was created with the Ligplot software [85].

Table 2
Selected automated docking results for the synthesized PCU derived hydroxy ether peptide and peptoid inhibitors and comparison to the experimental HIV–PR inhibition results. (All of the docked inhibitor–enzyme complex results are available in PDB format and are provided with the Supplementary material.)

Compound[a]	Binding energy[b] (kcal/mol)	IC_{50} (μM)
16-a[c]	−6.95	2
16-b[c]	−7.01	
17-a[c]	−7.10	1
17-b[c]	−7.74	
20-a[c]	−8.98	0.6
20-b[c]	−8.01	
21-a[c]	−6.54	60
21-b[c]	−5.92	
23-a[d]	−7.21	5
23-b[d]	−6.61	

[a] The stereochemistry for the cage peptide is 8-(R)-11-(R)-PCU-peptide for the "a" diastereomer and 8-(S)-11-(S)-PCU-peptide for the "b" diastereomer.
[b] Energy calculated from Autodock. The 3D structures of the docked complexes are available as Supplementary material.
[c] These two diastereomers were not separated and the IC_{50} values are for the mixture.
[d] These two enantiomers were not separated and the IC_{50} values are for the mixture.

after docking and the variation in orientation of these amino acids in the binding cavity was unnoticeable. Diastereomers of PCU peptides and peptoids were obtained from the coupling of the enantiopure short peptide or peptoids to the racemic PCU hydroxyl acid [33,34,57,84], Fig. 3a and b.

Docking routines of the new PCU–peptide inhibitors with the C-SA enzyme were performed. The binding energies of the docked diastereomeric PCU–peptide inhibitors have been tabulated (Table 2). The docking results are in reasonable agreement with the measured IC_{50} values.

In our previous reports [33,34] it was demonstrated that the chirality of the PCU cage is important for enhanced inhibition. The docking results in this study again confirm this observation [33,34]. This suggests that the diastereomers should ideally be separated when more promising cage peptide inhibitors are discovered.

Docking studies have clearly showed that conserved hydrogen bonds formed between the cage hydroxy ether moiety and Asp25/Asp25′ of the dimeric catalytic triad residues, Asp25-Thr26-Gly27 (A/B chains) (Figs. 4 and 5 and the Supplementary information). Such hydrogen bonds anchor the cage skeleton to the $S^1/S^{1'}$ subsite causing the adjacent amino acids to shift to the $S^2/S^{2'}$ and $S^3/S^{3'}$. This could explain the finding that less hydrophobic amino acids, such as valine, directly attached to the cage exhibited higher activity.

Even though docking calculations cannot provide insight on the dynamic inhibitor–enzyme interactions, they provided us with a general picture of the most energetically favorable binding orientation of inhibitors to the enzyme. To obtain further insight into the dynamic changes of the docked inhibitors within the enzyme active site pocket over time, the lowest energy docked complex of the inhibitor **20** was subjected to unconstrained MD simulations (2 ns).

The MD simulations clearly showed that the inhibitor easily fits into the active enzyme pocket. To assess the quality of our MD simulations, energetic and structural properties are monitored along the entire 2 ns MD trajectory of the complex. Fig. 6a presents the plot of the potential energy of the system as a function of time. The fluctuation of potential energy is less than 1000 kcal mol^{-1} over the course of the reaction.

The 2 ns averaged backbone RMSDs for the **20** enzyme complex is 1.16 Å and this is an indication that the generated MD trajectory of the complex is quite stable. The overall orientation of the
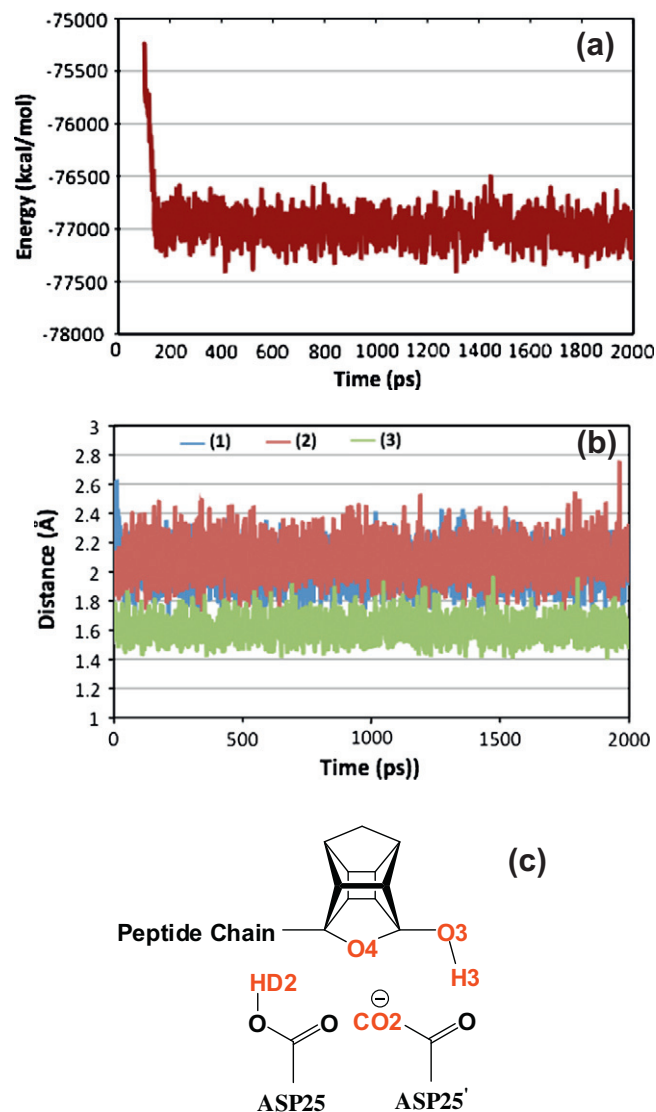

Fig. 6. (a) The potential energy of 20 C-SA HIV–PR complex observed in MD simulation as a function of time. (b) Selected distances obtained from MD simulations: (1) cage(O4)–Asp25(HD2), (2) cage(O3)–Asp25(HD2) and (3) cage(H3)–Asp25′(OD2). (c) Labeling of some atoms involved in hydrogen bond formation.

complex is preserved and very little movement of the PCU cage hydroxy ether inside the enzyme pocket is observed during the course of the MD run. However, slight changes in the orientation in the cage inhibitor peptide side chain were observed. As evident from the analysis of the hydrogen bond interactions along the MD trajectories, the inhibitor is forming hydrogen bonds between the cage hydroxy ether moiety and at least one of the two Asp25 carboxyl groups (Fig. 6c).

4. Conclusion

Pentacycloundecane derived hydroxy acid peptides have emerged as a new class of irreversible non-scissile ether bridge type isoters. The results demonstrate the possibility of employing the cage peptides as potential protease inhibitors. Docking and MD simulations suggest that the cage or part thereof occupies the $S^1/S^{1'}$ subsite. The incorporation of bulky substituents such as phenylalanine at the $S^2/S^{2'}$ and $S^3/S^{3'}$ subsites can alter the conformational

arrangement of the inhibitor which consequently reduces their binding affinity.

Further optimizations as well as in-depth structural and biological studies of the selected PCU derived-peptide/peptoid based protease inhibitors are the subject of ongoing investigations.

Acknowledgments

Appendix A. Supplementary material

Supplementary data associated with this article can be found, in the online version, at doi:10.1016/j.bioorg.2011.08.002.

References

[1] Report on the Global AIDS Epidemic, in: UNAIDS (2008), Joint United Nations Programme on HIV/AIDS (UNAIDS), (2008), pp. 1–31.
[2] P.M.D. Fitzgerald, J.P. Springer, Annual Review of Biophysics and Biophysical Chemistry 20 (1991) 299–320.
[3] M.L. West, D.P. Fairlie, Trends in Pharmacological Sciences 16 (1995) 67–75.
[4] E.K. Kick, J.A. Ellman, Journal of Medicinal Chemistry 38 (1995) 1427–1430.
[5] J.L. Martinez-Cajas, M.A. Wainberg, Antiviral Research 76 (2007) 203–221.
[6] R.E. Babine, S.L. Bender, Chemical Reviews 97 (1997) 1359–1472.
[7] A. Wlodawer, J. Vondrasek, Annual Review of Biophysics and Biomolecular Structure 27 (1998) 249–284.
[8] X.Y. Wu, P. Ohrngren, J.K. Ekegren, J. Unge, T. Unge, H. Wallberg, B. Samuelsson, A. Hallberg, M. Larhed, Journal of Medicinal Chemistry 51 (2008) 1053–1058.
[9] T. Lee, G.S. Laco, B.E. Torbett, H.S. Fox, D.L. Lerner, J.H. Elder, C.H. Wong, Proceedings of the National Academy of Sciences of the United States of America 95 (1998) 939–944.
[10] A. Velaquez-Campoy, S. Vega, E. Fleming, U. Bacha, Y. Sayed, H.W. Dirr, E. Freire, AIDS Reviews 5 (2003) 165–171.
[11] J.A. Partaledis, K. Yamaguchi, M. Tisdale, E.E. Blair, C. Falcione, B. Maschera, R.E. Myers, S. Pazhanisamy, O. Futer, A.B. Cullinan, C.M. Stuver, R.A. Byrn, D.J. Livingston, Journal of Virology 69 (1995) 5228–5235.
[12] A. Staszewska, P. Stefanowicz, Z. Szewczuk, Tetrahedron Letters 46 (2005) 5525–5528.
[13] K.B. Brookes, P.W. Hickmott, K.K. Jutle, C.A. Schreyer, South African Journal of Chemistry-Suid-Afrikaanse Tydskrif Vir Chemie 45 (1992) 8–11.
[14] W.J. Geldenhuys, S.F. Malan, J.R. Bloomquist, A.P. Marchand, C.J. Van der Schyf, Medicinal Research Reviews 25 (2005) 21–48.
[15] K. Gerzon, D. Kau, Journal of Medicinal Chemistry 10 (1967) 189–199.
[16] F.M. Ito, J.M. Petroni, D.P. de Lima, A. Beatriz, M.R. Marques, M.O. de Moraes, L.V. Costa-Lotufo, R.C. Montnegro, H.I.F. Magalhaes, C.D.O. Pessoa, Molecules 12 (2007) 271–282.
[17] D. Ranganathan, V. Haridas, K.P. Madhusudanan, R. Roy, R. Nagaraj, G.B. John, M.B. Sukhaswami, Angewandte Chemie-International Edition in English 35 (1996) 1105–1107.
[18] E. Grobler, A. Grobler, C.J. Van der Schyf, S.F. Malan, Bioorganic & Medicinal Chemistry 14 (2006) 1176–1181.
[19] D.W. Oliver, T.G. Dekker, F.O. Snyckers, T.G. Fourie, Journal of Medicinal Chemistry 34 (1991) 851–854.
[20] D.W. Oliver, T.G. Dekker, F.O. Snyckers, European Journal of Medicinal Chemistry 26 (1991) 375–379.
[21] V. Gokul, H.G. Kruger, T. Govender, L. Fourie, T.D. Power, Journal of Molecular Structure: Theochem 672 (2004) 119–125.
[22] K. Bisetty, J. Gomez-Catalan, C. Aleman, E. Giralt, H.G. Kruger, J.J. Perez, Journal of Peptide Science 10 (2004) 274–284.
[23] K. Bisetty, J.G. Catalan, H.G. Kruger, J.J. Perez, Journal of Molecular Structure: Theochem 731 (2005) 127–137.
[24] K. Bisetty, F.J. Corcho, J. Canto, H.G. Kruger, J.J. Perez, Journal of Peptide Science 12 (2006) 92–105.
[25] K. Bisetty, P. Govender, H.G. Kruger, Biopolymers 81 (2006) 339–349.
[26] K. Bisetty, F.J. Corcho, J. Canto, H.G. Kruger, J.J. Perez, Journal of Molecular Structure: Theochem 759 (2006) 145–157.
[27] H.G. Kruger, P. Mdluli, T.D. Power, T. Raasch, A. Singh, Journal of Molecular Structure: Theochem 771 (2006) 165–170.
[28] K. Bisetty, F.J. Corcho, J. Canto, H.G. Kruger, J.J. Perez, Journal of Molecular Structure: Theochem 770 (2006) 221–228.
[29] T. Singh, K. Bisetty, H.G. Kruger, Trends and Perspectives in Modern Computational Science 7 (2006) 511–514.
[30] K. Bisetty, H.G. Kruger, J.J. Perez, Molecular Simulation 33 (2007) 1105–1108.
[31] F. Albericio, P.I. Arvidson, K. Bisetty, E. Giralt, T. Govender, S. Jali, P. Kongsaeree, H.G. Kruger, S. Prabpai, Chemical Biology & Drug Design 71 (2008) 125–130.
[32] P. Singh, K. Bisetty, P. Govender, G. Kruger, South African Journal of Chemistry-Suid-Afrikaanse Tydskrif Vir Chemie 64 (2011) 49–56.
[33] M.M. Makatini, K. Petzold, S.N. Sriharsha, M.E.S. Soliman, B. Honarparvar, P.I. Arvidsson, Y. Sayed, P. Govender, G.E.M. Maguire, H.G. Kruger, T. Govender, Bioorganic & Medicinal Chemistry Letters 21 (2011) 2274–2277.
[34] M.M. Makatini, K. Petzold, S.N. Sriharsha, N. Ndlovu, M.E.S. Soliman, B. Honarparvar, R. Parboosing, A. Naidoo, P.I. Arvidsson, Y. Sayed, P. Govender, G.E.M. Maguire, H.G. Kruger, T. Govender, European Journal of Medicinal Chemistry, in press, 2011.
[35] H.G. Kruger, P.S. Mdluli, Structural Chemistry 17 (2006) 121–125.
[36] O.K. Onajole, T. Govender, M. Makatini, H.G. Kruger, Structural Chemistry 19 (2008) 719–726.
[37] O.K. Onajole, T. Govender, M. Makatini, H.G. Kruger, Magnetic Resonance in Chemistry 46 (2008) 1007–1014.
[38] O.K. Onajole, P. Govender, T. Govender, G.E.M. Maguire, H.G. Kruger, Structural Chemistry 20 (2009) 1067–1076.
[39] M.S. Altaib, P.I. Arvidsson, T. Govender, G.E.M. Maguire, M. Makatini, O.K. Onajole, H.G. Kruger, Magnetic Resonance in Chemistry 48 (2010) 435–442.
[40] O.K. Onajole, M.M. Makatini, P. Govender, T. Govender, G.E.M. Maguire, H.G. Kruger, Magnetic Resonance in Chemistry 48 (2010) 249–255.
[41] O.K. Onajole, P. Govender, T. Govender, G.E.M. Maguire, H.G. Kruger, Structural Chemistry 21 (2010) 1203–1209.
[42] O.K. Onajole, X.V. Belewa, Y. Coovadia, T. Govender, H.G. Kruger, G.E.M. Maguire, D. Naidu, B. Somai, N. Singh, P. Govender, Medicinal Chemistry Research, in press, doi:10.1007/s00044-010-9490-3.
[43] O.K. Onajole, K. Govender, P. Govender, P.D. van Helden, H.G. Kruger, G.E.M. Maguire, K. Muthusamy, M. Pillay, I. Wiid, T. Govender, European Journal of Medicinal Chemistry 44 (2009) 4297–4305.
[44] O.K. Onajole, P. Govender, P.D. van Helden, H.G. Kruger, G.E.M. Maguire, I. Wiid, T. Govender, European Journal of Medicinal Chemistry 45 (2010) 2075–2079.
[45] O.K. Onajole, Y. Coovadia, T. Govender, H.G. Kruger, G.E.M. Maguire, D. Naidu, N. Singh, P. Govender, Chemical Biology & Drug Design 77 (2011) 295–299.
[46] C. Adessi, C. Soto, Current Medicinal Chemistry 9 (2002) 963–978.
[47] V.J. Hruby, P.M. Balse, Current Medicinal Chemistry 7 (2000) 945–970.
[48] R.N. Zuckermann, J.M. Kerr, S.B.H. Kent, W.H. Moos, Journal of the American Chemical Society 114 (1992) 10646–10647.
[49] S.M. Miller, R.J. Simon, S. Ng, R.N. Zuckermann, J.M. Kerr, W.H. Moos, Bioorganic & Medicinal Chemistry Letters 4 (1994) 2657–2662.
[50] S.M. Miller, R.J. Simon, S. Ng, R.N. Zuckermann, J.M. Kerr, W.H. Moos, Drug Development Research 35 (1995) 20–32.
[51] R.J. Simon, R.S. Kania, R.N. Zuckermann, V.D. Huebner, D.A. Jewell, S. Banville, S. Ng, L. Wang, S. Rosenberg, C.K. Marlowe, D.C. Spellmeyer, R.Y. Tan, A.D. Frankel, D.V. Santi, F.E. Cohen, P.A. Bartlett, Proceedings of the National Academy of Sciences of the United States of America 89 (1992) 9367–9371.
[52] J.C. Clemente, R.M. Coman, M.M. Thiaville, L.K. Janka, J.A. Jeung, S. Nukoolkarn, L. Govindasamy, M. Agbandje-McKenna, R. McKenna, W. Leelamanit, M.M. Goodenow, B.M. Dunn, Biochemistry 45 (2006) 5468–5477.
[53] A. Brik, C.H. Wong, Organic & Biomolecular Chemistry 1 (2003) 5–14.
[54] D.J. Kempf, K.C. Marsh, J.F. Denissen, E. McDonald, S. Vasavanonda, C.A. Flentge, B.E. Green, L. Fino, C.H. Park, X.P. Kong, N.E. Wideburg, A. Saldivar, L. Ruiz, W.M. Kati, H.L. Sham, T. Robins, K.D. Stewart, A. Hsu, J.J. Plattner, J.M. Leonard, D.W. Norbeck, Proceedings of the National Academy of Sciences of the United States of America 92 (1995) 2484–2488.
[55] J.D.A. Tyndall, R.C. Reid, D.P. Tyssen, D.K. Jardine, B. Todd, M. Passmore, D.R. March, L.K. Pattenden, D.A. Bergman, D. Alewood, S.H. Hu, P.F. Alewood, C.J. Birch, J.L. Martin, D.P. Fairlie, Journal of Medicinal Chemistry 43 (2000) 3495–3504.
[56] T.W. Ridky, C.E. Cameron, J. Cameron, J. Leis, T. Copeland, A. Wlodawer, T.I. Weber, R.W. Harrison, Journal of Biological Chemistry 271 (1996) 4709–4717.
[57] F.J.C. Martins, A.M. Viljoen, H.G. Kruger, P.L. Wessels, Tetrahedron 49 (1993) 6527–6532.
[58] A.K. Ghosh, W.J. Thompson, S.P. McKee, T.T. Duong, T.A. Lyle, J.C. Chen, P.L. Darke, J.A. Zugay, E.A. Emini, Journal of Medicinal Chemistry 36 (1993) 292–294.
[59] A.K. Ghosh, J.F. Kincaid, W.H. Cho, D.E. Walters, K. Krishnan, K.A. Hussain, Y. Koo, H. Cho, C. Rudall, L. Holland, J. Buthod, Bioorganic & Medicinal Chemistry Letters 8 (1998) 687–690.
[60] A.K. Ghosh, S. Leshchenko, M. Noetzel, Journal of Organic Chemistry 69 (2004) 7822–7829.
[61] S. Mosebi, L. Morris, H.W. Dirr, Y. Sayed, Journal of Virology 82 (2008) 11476–11479.
[62] H.M. Yu, S.T. Chen, K.T. Wang, Journal of Organic Chemistry 57 (1992) 4781–4784.
[63] T. Yamamoto, P. Nair, N.E. Jacobsen, P. Davis, S.-w. Ma, E. Navratilova, S. Moye, J. Lai, H.I. Yamamura, T.W. Vanderah, F. Porreca, V.J. Hruby, Journal of Medicinal Chemistry 51 (2008) 6334–6347.

[64] Avogadro: An Open-Source Molecular Builder and Visualization Tool. Version 1.0.0. <http://avogadro.openmolecules.net/>.

[65] T.A. Soares, D.S. Goodsell, R. Ferreira, A.J. Olson, J.M. Briggs, Journal of Molecular Recognition 13 (2000) 146–156.

[66] T.M. Frimurer, G.H. Peters, L.F. Iversen, H.S. Andersen, N.P.H. Moller, O.H. Olsen, Biophysical Journal 84 (2003) 2273–2281.

[67] C.W. Locuson, P.M. Gannett, R. Ayscue, T.S. Tracy, Journal of Medicinal Chemistry 50 (2007) 1158–1165.

[68] R. Smith, I.M. Brereton, R.Y. Chai, S.B.H. Kent, Nature Structural Biology 3 (1996) 946–950.

[69] G.M. Morris, D.S. Goodsell, R.S. Halliday, R. Huey, W.E. Hart, R.K. Belew, A.J. Olson, Journal of Computational Chemistry 19 (1998) 1639–1662.

[70] M.F. Sanner, Journal of Molecular Graphics & Modelling 17 (1999) 57–61.

[71] R. Huey, G.M. Morris, A.J. Olson, D.S. Goodsell, Journal of Computational Chemistry 28 (2007) 1145–1152.

[72] J. Wang, W. Wang, P.A. Kollman, D.A. Case, Journal of Molecular Graphics and Modelling 25 (2006) 247–260.

[73] D.A. Case, T.E. Cheatham, T. Darden, H. Gohlke, R. Luo, K.M. Merz, A. Onufriev, C. Simmerling, B. Wang, R.J. Woods, Journal of Computational Chemistry 26 (2005) 1668–1688.

[74] J.M. Wang, R.M. Wolf, J.W. Caldwell, P.A. Kollman, D.A. Case, Journal of Computational Chemistry 25 (2004) 1157–1174.

[75] Y. Duan, C. Wu, S. Chowdhury, M.C. Lee, G.M. Xiong, W. Zhang, R. Yang, P. Cieplak, R. Luo, T. Lee, J. Caldwell, J.M. Wang, P.A. Kollman, Journal of Computational Chemistry 24 (2003) 1999–2012.

[76] W.L. Jorgensen, J. Chandrasekhar, J.D. Madura, R.W. Impey, M.L. Klein, Journal of Chemical Physics 79 (1983) 926–935.

[77] U. Essmann, L. Perera, M.L. Berkowitz, T. Darden, H. Lee, L.G. Pedersen, Journal of Chemical Physics 103 (1995) 8577–8593.

[78] J.P. Ryckaert, G. Ciccotti, H.J.C. Berendsen, Journal of Computational Physics 23 (1977) 327–341.

[79] H.J.C. Berendsen, J.P.M. Postma, W.F. van Gunsteren, A. DiNola, J.R. Haak, Journal of Chemical Physics 81 (1984) 3684–3690.

[80] R.C. Cookson, E. Crundwell, R.R. Hill, J. Hudec, Journal of the Chemical Society (1964) 3062–3075.

[81] A.P. Marchand, R.W. Allen, Journal of Organic Chemistry 39 (1974) 1596.

[82] A.P. Marchand, Advances in Theoretically Interesting Molecules 1 (1989) 357–399.

[83] O.A. Gutierrez, E. Salas, Y. Hernandez, E.A. Lissi, G. Castrillo, O. Reyes, H. Garay, A. Aguilar, B. Garcia, A. Otero, M.A. Chavez, C.A. Duarte, Analytical Biochemistry 307 (2002) 18–24.

[84] F.J.C. Martins, A.M. Viljoen, H.G. Kruger, J.A. Joubert, Tetrahedron 49 (1993) 9573–9580.

[85] A.C. Wallace, R.A. Laskowski, J.M. Thornton, Protein Engineering 8 (1995) 127–134.